PROJECT REPORT

HYBRID MULTI-OUTPUT QUADRATIC BOOST CONVERTER

Under the Guidance of:
Dr. R K Singh

Submitted by:

Parimey D Patil 15085046

I. INTRODUCTION:

In the recent years, Hybrid Converters have gained a lot of attention due to their ability to provide simultaneous multi outputs utilizing a single dc source. Hybrid Converters are mostly used in the AC/DC Micro Grid Applications where the load requirement is both AC as well as DC. Earlier, separate converters were used to serve this purpose. However, with the recent developments it is possible to achieve this purpose with a single converter hence reducing components and increasing reliability.

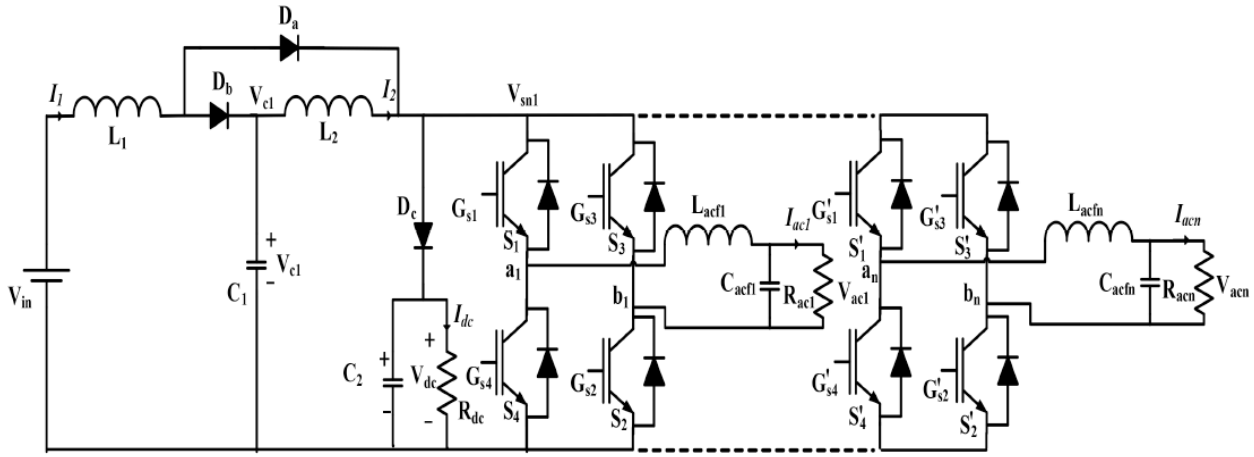

Fig. 1 Circuit Diagram of the Multi-Output Converter

II. About the Multi-Output Topology

The topology presented here is capable of giving single DC output and *n* number of AC outputs from a single DC Source. The nature of DC output is step-up type and that of AC outputs is both step-up and step-down. Thus, this topology can give boost DC output and both buck and boost AC outputs. The Quadratic Boost stage provides higher DC voltage gain than conventional boost converter in lower shoot-through duty cycle. It also provides inherent shoot-through protection. In this project only two AC and one DC outputs have been considered and experimentally validated.

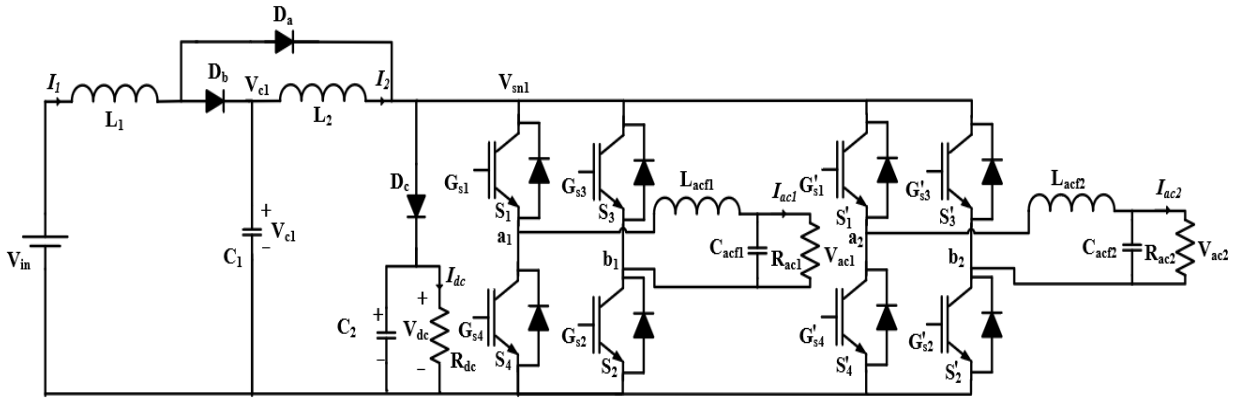

Fig. 2 Circuit Diagram of the Multi-Output Converter (2 AC and 1 DC outputs)

III. Steady State Analysis

The converter mainly operates in two intervals
1) Shoot-through Interval (D_{st})
2) Non shoot-through Interval ($1-D_{st}$)

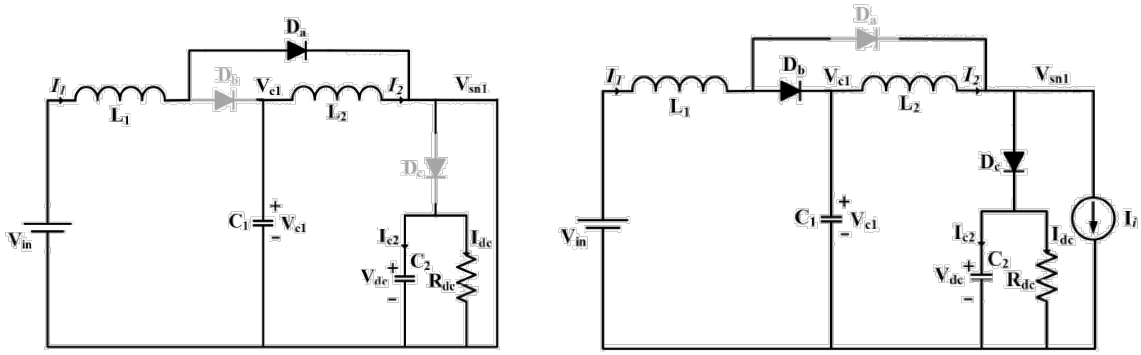

Fig. 3 (a) Interval 1 (b) Interval 2

1) Shoot through Interval

This interval stays for $D_{st}T_s$ period in each switching cycle. In this interval either of the two legs of all the inverters are switched ON depending on the PWM. During this interval diode D_a and either switches S_1-S_4 or S_2-S_3 of H-bridge network are conducting and the diodes D_b, D_c are reverse biased. Both the inductors L_1 and L_2 are charged in this interval. Capacitors C_1 and C_2 discharge and C_2 supplies the current to the load.

The instantaneous voltage and current expressions for shoot-through interval

$$L_1 \frac{di_1}{dt} = v_{in} \qquad L_2 \frac{di_2}{dt} = v_{C1}$$

$$C_1 \frac{dv_{C1}}{dt} = -i_2 \qquad C_2 \frac{dv_{C2}}{dt} = -i_{dc} = -\frac{v_{C2}}{R_{dc}}$$

2) Non shoot-through Interval

This interval stays for $(1\text{-}D_{st})T_s$ period in each switching cycle. In this interval all the inverters are either in the power stage or zero stage depending on the modulation index of that particular inverter and the PWM. During this interval diodes D_b-D_c and either switches S_1-S_2 or S_3-S_4 or S_1-S_3 or S_2-S_4 of H-bridge network are conducting and diode D_a is reverse biased. Both the inductors L_1 and L_2 discharge in this interval. Capacitors C_1 and C_2 gets charged in this interval. The total current flowing through the inverters in this interval can be represented by I_i.

The instantaneous voltage and current expressions for non-shoot-through interval

$$L_1 \frac{di_1}{dt} = v_{in} - v_{C1} \qquad L_2 \frac{di_2}{dt} = v_{C1} - v_{C2}$$

$$C_1 \frac{dv_{C1}}{dt} = i_1 - i_2 \qquad C_2 \frac{dv_{C2}}{dt} = i_2 - i_{dc} - i_i$$

Applying volt-second balance on the inductors L_1 and L_2, the following mathematical relations are achieved

$$V_{c1} = \frac{V_{in}}{(1 - D_{st})}$$

$$V_{c2} = \frac{V_{c1}}{(1 - D_{st})} = \frac{V_{in}}{(1 - D_{st})^2}$$

$$V_{dc} = V_{C2} = \frac{V_{in}}{(1 - D_{st})^2}$$

Applying charge-sec balance on the capacitors C_1 and C_2 the following mathematical relations are achieved

$$I_1 = \frac{I_2}{(1 - D_{st})}$$

$$I_2 = I_i + \frac{I_{dc}}{(1 - D_{st})}$$

$$I_{in} = I_1 = \frac{I_i}{(1 - D_{st})} + \frac{I_{dc}}{(1 - D_{st})^2}$$

From the steady state equations, it can be observed that the DC boost factor is

$$\mathrm{B} = \frac{V_{dc}}{V_{in}} = \frac{1}{(1 - D_{st})^2}$$

The AC peak of different inverters is given by the relation

$$V_{acpki} = M_i \times V_{dc} = \frac{M_i V_{in}}{(1 - D_{st})^2}$$

where V_{acpki} and M_i represents the AC peak and modulation index respectively of the i^{th} inverter.

The PWM used for this topology has the following constraint between the Modulation Index(M_i) and the Duty Ratio(D_{st})

$$D_{st} + M_i \leq 1$$

for all the inverters.

The output DC power (P_{dc}) is given by the relation

$$P_{dc} = \frac{V_{dc}^2}{R_{dc}} = \frac{V_{in}^2}{R_{dc}(1 - D_{st})^4}$$

The output AC power (P_{ac}) is given by the relation

$$P_{ac} = \frac{V_{ac1}^2}{R_{ac1}} + \frac{V_{ac2}^2}{R_{ac2}} = \frac{V_{acpk1}^2}{2R_{ac1}} + \frac{V_{acpk2}^2}{2R_{ac2}} = \frac{V_{in}^2}{2(1 - D_{st})^4}\left(\frac{M_1^2}{R_{ac1}} + \frac{M_2^2}{R_{ac2}}\right)$$

Voltage Stress across different components in both the intervals:

Parameters	Shoot-through state	Non-Shoot-through state
V_{L1}	V_{in}	$\frac{-D_{st}V_{in}}{1-D_{st}}$
V_{L2}	$\frac{V_{in}}{1-D_{st}}$	$\frac{-D_{st}V_{in}}{(1-D_{st})^2}$
V_{C1}	$\frac{V_{in}}{1-D_{st}}$	$\frac{V_{in}}{1-D_{st}}$
V_{C2}	$\frac{V_{in}}{(1-D_{st})^2}$	$\frac{V_{in}}{(1-D_{st})^2}$
V_{Da}	0	$\frac{-D_{st}V_{in}}{(1-D_{st})^2}$
V_{Db}	$\frac{-V_{in}}{1-D_{st}}$	0
V_{Dc}	$\frac{-V_{in}}{(1-D_{st})^2}$	0
V_{Si}	0	$\frac{V_{in}}{(1-D_{st})^2}$

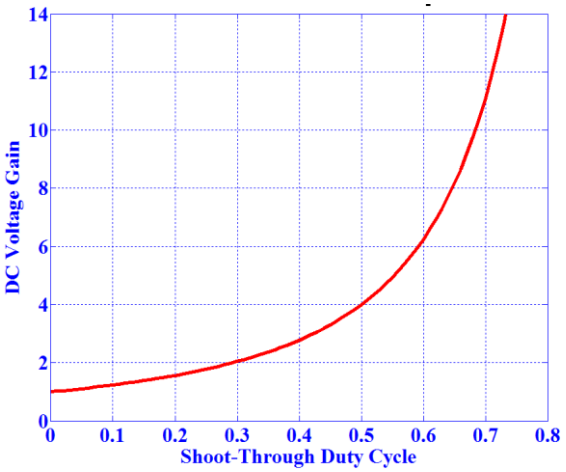

Fig. 4 Variation of DC voltage gain with D_{st}

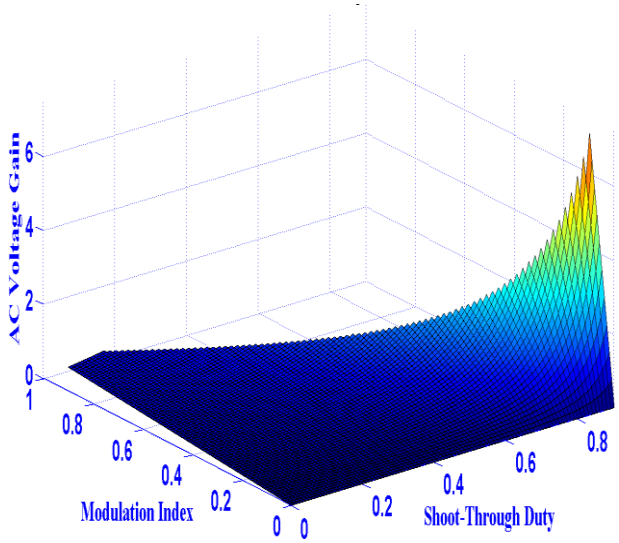

Fig. 5 Variation of ac rms voltage with M and D_{st}

IV. PWM Technique and Gating Waveforms

Hybrid PWM technique is used for modulating the ac outputs of the quadratic boost derived hybrid multi-output converter. In hybrid PWM technique, one switching cycle containing both power as well as the shoot-through interval is implemented.

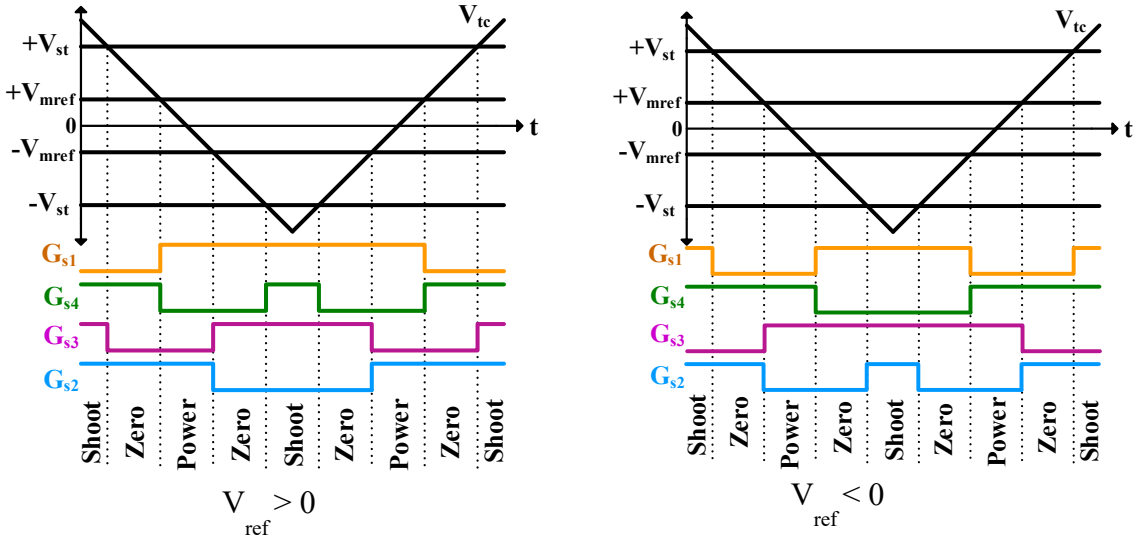

Fig. 6

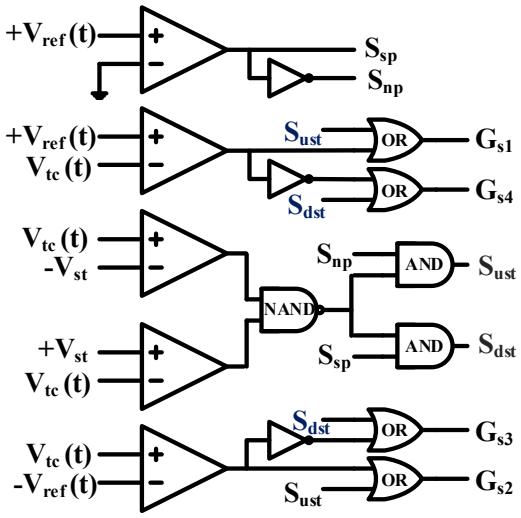

Fig. 7 Analogue representation of PWM Logic

V. Small Signal Analysis

The simplified equivalent circuit of converter is shown.

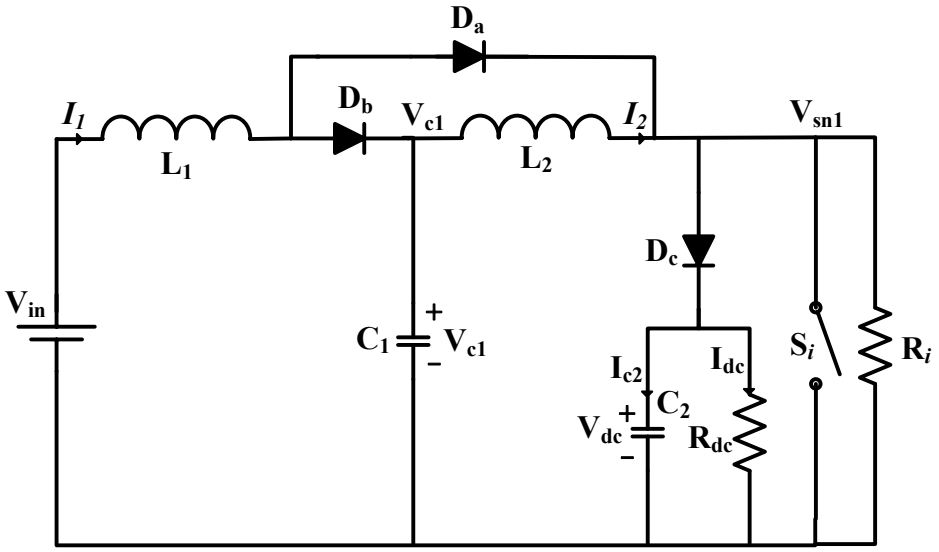

Fig. 8 Simplified circuit diagram for hybrid multi-output converter

From the state space averaging technique, the following differential equations are obtained

$$L_1 \frac{d\tilde{\imath}_1}{dt} = \tilde{v}_{in} - \left(1 - \tilde{d}_{st}\right)\tilde{v}_{C1}$$

$$L_2 \frac{d\tilde{\imath}_2}{dt} = \tilde{v}_{C1} - (1 - \tilde{d}_{st})\tilde{v}_{C2}$$

$$C_1 \frac{d\tilde{v}_{C1}}{dt} = (1 - \tilde{d}_{st})\tilde{\imath}_1 - \tilde{\imath}_2$$

$$C_2 \frac{d\tilde{v}_{C2}}{dt} = (1 - \tilde{d}_{st})\tilde{\imath}_2 - \frac{\tilde{v}_{C2}}{R_{dc}} - (1 - \tilde{d}_{st})\frac{\tilde{v}_{C2}}{R_i}$$

After applying the perturbation and linearization techniques the whole model can be written in the form

$$\mathrm{K}\hat{\dot{x}} = \mathrm{A}\hat{x} + \mathrm{B}\hat{v}_{in} + [(\mathrm{A}_1 - \mathrm{A}_2)\mathrm{X} + (\mathrm{B}_1 - \mathrm{B}_2)\mathrm{V}_{\mathrm{in}}]\widehat{d_{st}}$$

$$\hat{\dot{x}} = (\mathrm{K}^{-1}\mathrm{A})\hat{x} + (\mathrm{K}^{-1}\mathrm{B})\hat{v}_{in} + [\mathrm{K}^{-1}(\mathrm{A}_1 - \mathrm{A}_2)\mathrm{X} + (\mathrm{B}_1 - \mathrm{B}_2)\mathrm{V}_{\mathrm{in}}]\widehat{d_{st}}$$

$$K = \begin{bmatrix} L_1 & 0 & 0 & 0 \\ 0 & L_2 & 0 & 0 \\ 0 & 0 & C_1 & 0 \\ 0 & 0 & 0 & C_2 \end{bmatrix}; \quad A_1 = \begin{bmatrix} 0 & 0 & 0 & 0 \\ 0 & 0 & 1 & 0 \\ 0 & -1 & 1 & 0 \\ 0 & 0 & 0 & -1/R_{dc} \end{bmatrix};$$

$$A_2 = \begin{bmatrix} 0 & 0 & -1 & 0 \\ 0 & 0 & 1 & -1 \\ 1 & -1 & 1 & 0 \\ 0 & 1 & 0 & -\frac{1}{R_i} - \frac{1}{R_{dc}} \end{bmatrix}$$

$$B_1 = [1 \quad 0 \quad 0 \quad 0]^T \; ; \; B_2 = [1 \quad 0 \quad 0 \quad 0]^T ;$$

$$A = A_1 D_{st} + A_2(1 - D_{st})$$

$$= \begin{bmatrix} 0 & 1 & -(1 - D_{st}) & 0 \\ 0 & 0 & 1 & -(1 - D_{st}) \\ -(1 - D_{st}) & -1 & 0 & 0 \\ 0 & -(1 - D_{st}) & 0 & -\frac{(1 - D_{st})}{R_i} - \frac{1}{R_{dc}} \end{bmatrix}$$

$$B = B_1 D_{st} + B_2(1 - D_{st}) = [1 \quad 0 \quad 0 \quad 0]^T$$

$$X = [I_1 \quad I_2 \quad V_{C1} \quad V_{C2}]^T$$

$$\dot{x} = \frac{d}{dt}[i_1 \quad i_2 \quad v_{C1} \quad v_{C2}]^T$$

$$\hat{\dot{x}} = S_1 \hat{x} + S_2 \hat{v}_{in} + S_3 \widehat{d_{st}}$$

$$S_1 = (K^{-1}A); \; S_2 = (K^{-1}B); \; S_3 = K^{-1}[(A_1 - A_2)X + (B_1 - B_2)V_{in}]$$

The control to output transfer function of the converter is given by

$$\frac{\hat{v}_o}{\hat{d}_{st}} = [0 \quad 0 \quad 0 \quad 1 \quad 0][sI - S_1]^{-1} S_3$$

$$= \frac{A's^3 + B's^2 + C's + D'}{A''s^4 + B''s^3 + C''s^2 + D''s + E''}$$

$$A' = C_1 L_1 L_2 R_{dc} V_{C2} - C_1 L_1 L_2 I_2 R_i$$

$$B' = C_1 L_1 (1 - D_{st}) R_{dc} R_i V_{C2}$$

$$A'' = C_1 C_2 L_1 L_2 R_{dc} R_i$$

$$B'' = C_1 L_1 L_2 R_i + C_1 (1 - D_{st}) L_1 L_2 R_{dc};$$

$$C' = L_1 R_{dc} V_{C2} - L_1 R_{dc} R_i I_2 + L_2 R_{dc} V_{C2} (1 - D_{st})^2 - L_1 R_{dc} R_i I_1 (1 - D_{st}) - L_2 R_{dc} R_i I_2 (1 - D_{st})^2$$

$$D' = R_{dc} R_i V_{C2} (1 - D_{st})^3 + R_{dc} R_i V_{C1} (1 - D_{st})^2$$

$$C'' = C_1 L_1 R_{dc} R_i + C_1 L_1 (1 - D_{st})^2 R_{dc} R_i + C_2 L_2 (1 - D_{st})^2 R_{dc} R_i,$$

$$D'' = L_2 R_{dc} (1 - D_{st})^3 + L_2 R_i (1 - D_{st})^2 + L_1 R_{dc} (1 - D_{st}) + L_1 R_i,$$

$$E'' = R_{dc} (1 - D_{st})^4 R_i$$

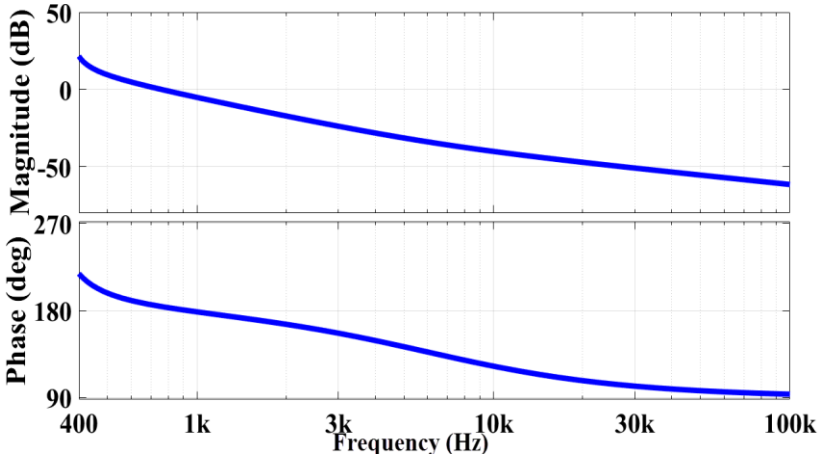

Fig. 9 Open Loop Frequency Response

VI. Experimental Validation

The hybrid multi-output converter has been validated on a 250 W prototype.

Following are the PWM waveforms for positive sine reference in positive half and negative half.

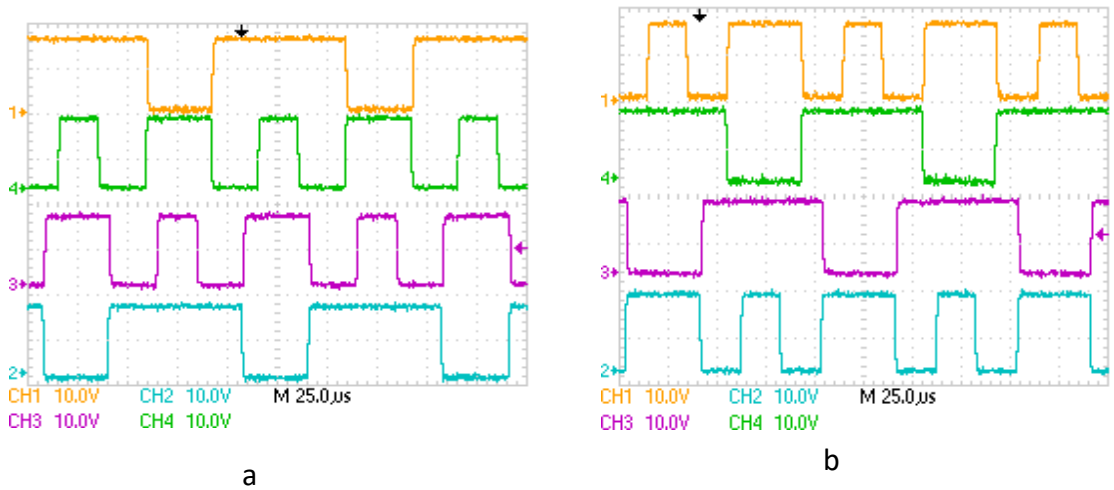

a b

Fig. 10 PWM waveform when (a) V_{ref} >0 , (b) V_{ref} <0

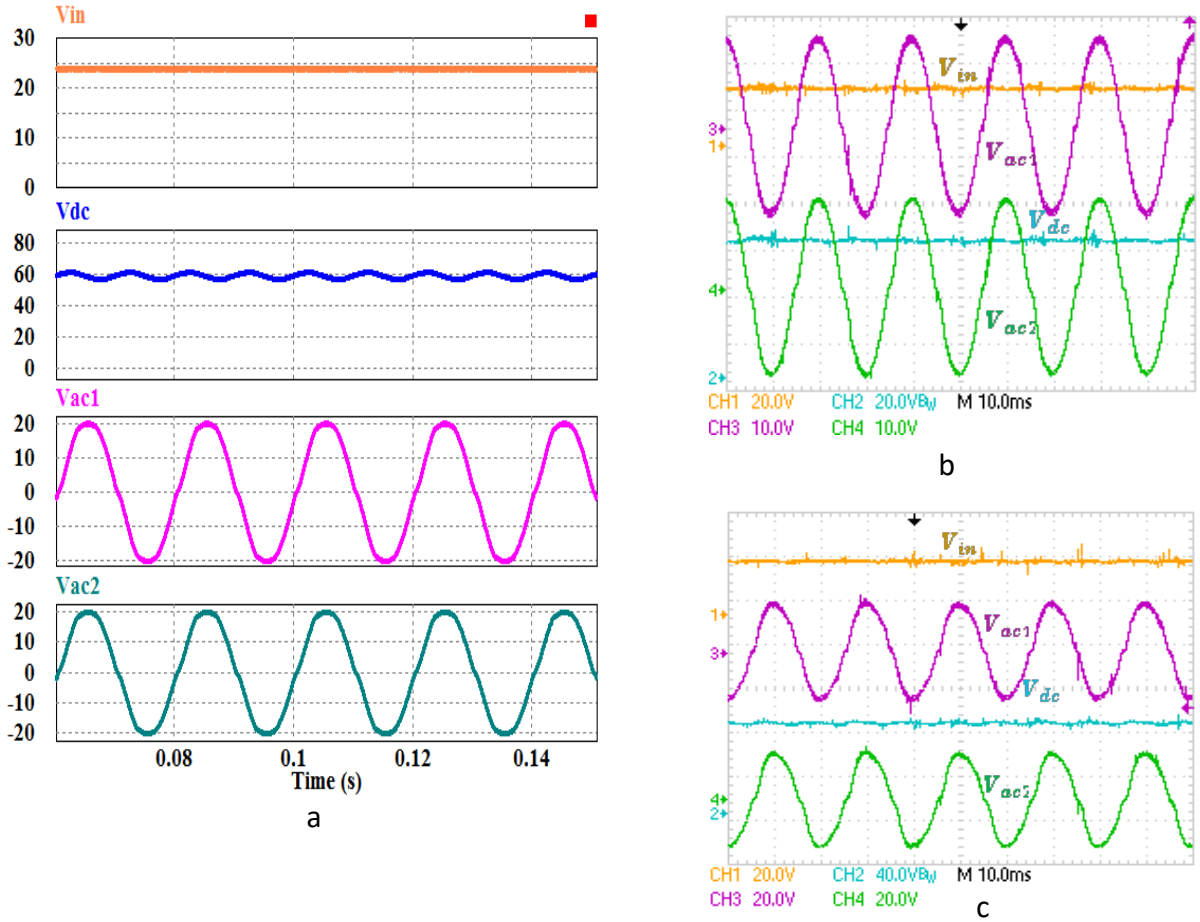

a b c

Fig. 11 (a)Steady State simulation result, (b) Steady state experimental result for D_{st} = 0.4 and M = 0.5, (c) Steady state experimental result for D_{st} = 0.5 and M = 0.4

Steady state simulation results of the converter for D_{st}= 0.4 and M=0.5 are shown in Fig. 11(a). It is observed from the figure that two ac output voltages V_{ac1} = 40.4 V (pk-pk) and V_{ac2} = 40.4 V (pk-pk) along with dc output voltage V_{dc} = 59.4 V are obtained from the input voltage V_{in} = 24 V. Experimental verifications are shown in

Fig 11 (b) and (c) for D_{st}= 0.4, M=0.5 and D_{st}= 0.5, M=0.4 respectively. From the Fig. 11 (b), it can be observed that two ac output voltages V_{ac1} = 39.4V (pk-pk) and V_{ac2} = 39.0 V (pk-pk) along with dc output voltage V_{dc} = 57.12 V are obtained for the input voltage V_{in} = 24 V. Similarly, it can be observed from Fig. 11 (c), that the proposed converter gives two ac output voltages V_{ac1} = 47.6 V (pk-pk) and V_{ac2} = 46.4 V (pk-pk) along with dc output voltage V_{dc} = 82.2V for the input voltage V_{in} = 24V. The simulation and experimental results confirm the steady state behavior of the multi-output topology for different values of D_{st} and M.

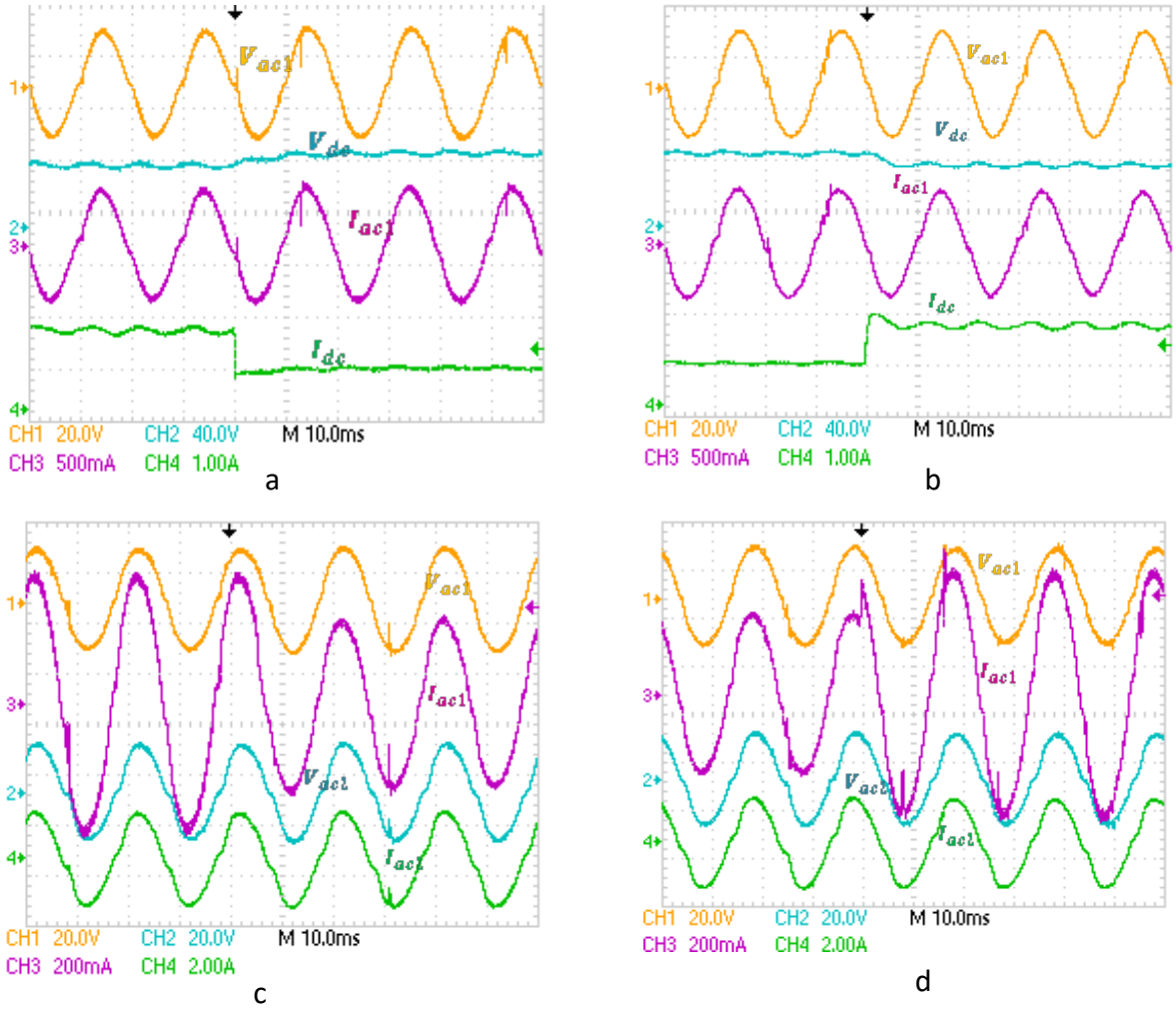

Fig. 12 Dynamic response of the converter, a) Step down change in the dc load current, b) Step up change in the dc load current, c) Step down change in the ac load current, d) Step up change in the ac load current

The dynamic behaviour of the converters is verified in open loop condition with the step change in the loads and the results are shown in Fig.12. Fig. 12a shows the response of the converter for step down dc load (from I_{dc} = 1.65 A to = 800 mA) variation by keeping the ac loads constant. It is evident from Fig. 12a that that dc load

step down operation, there is small variation in the dc load voltage (V_{dc}) and no variations in the ac output voltage and current. Similarly, Fig. 12b shows the step up dc load (from I_{dc} = 800 mA to 1.65 A) variation by keeping the ac loads constant. It can be observed from the Fig. 12b, that for dc step up operation, there is a small variation in the dc load voltage (V_{dc}) and no variations in the ac output voltage (V_{ac1}) and current (I_{ac1}). Fig. 12c shows the response of the converter for step down ac load (from I_{ac1} = 1.1 A to = 610 mA) variation while keeping the dc load constant. It is clear from Fig. 12c that for a step down operation in one of the ac loads there is no variation in ac load voltages ($V_{ac1} and\ V_{ac2}$) and other ac load current (I_{ac2}). Similarly, Fig.12d shows the step up ac load (from I_{ac1} = 610 mA to = 1.1 A) variation while keeping the dc load constant. It is clear from Fig. 12d that for a step up operation in one of the ac loads there is no variation in ac load voltages ($V_{ac1} and\ V_{ac2}$) and other ac load current (I_{ac2}). An important observation is noticed that dc load voltage (V_{dc}) and currents (I_{dc}) are not affected while dynamic change in ac loads.

VII. Conclusion

The Quadratic Boost Derived Hybrid Multi-Output Converter is capable of giving one DC and two AC outputs using a single DC source. Due to the quadratic behavior of the hybrid multi-output converter, high gain is achieved on low operating shoot-through duty cycle. The converter has higher power density and improved reliability due to inherent shoot-through protection. The simulation and experimental results are presented and the performance of the converter is validated using a 250 W prototype.